ASTROBIOLOGY
Volume 7, Number 2, 2007

DOI: 10.1089/ast.2006.0039

Research Paper

Rainbows, Polarization, and the Search for Habitable Planets

JEREMY BAILEY

ABSTRACT

Current proposals for the characterization of extrasolar terrestrial planets rest primarily on the use of spectroscopic techniques. While spectroscopy is effective in detecting the gaseous components of a planet's atmosphere, it provides no way of detecting the presence of liquid water, the defining characteristic of a habitable planet. In this paper, I investigate the potential of an alternative technique for characterizing the atmosphere of a planet using polarization. By looking for a polarization peak at the "primary rainbow" scattering angle, it is possible to detect the presence of liquid droplets in a planet's atmosphere and constrain the nature of the liquid through its refractive index. Single scattering calculations are presented to show that a well-defined rainbow scattering peak is present over the full range of likely cloud droplet sizes and clearly distinguishes the presence of liquid droplets from solid particles such as ice or dust. Rainbow scattering has been used in the past to determine the nature of the cloud droplets in the Venus atmosphere and by the POLarization and Directionality of Earth Reflectances (POLDER) instrument to distinguish between liquid and ice clouds in the Earth atmosphere. While the presence of liquid water clouds does not guarantee the presence of water at the surface, this technique could complement spectroscopic techniques for characterizing the atmospheres of potential habitable planets. The disk-integrated rainbow peak for Earth is estimated to be at a degree of polarization of 12.7% or 15.5% for two different cloud cover scenarios. The observation of this rainbow peak is shown to be feasible with the proposed Terrestrial Planet Finder Coronograph mission in similar total integration times to those required for spectroscopic characterization. Key Words: Polarization—Planetary atmospheres—Extrasolar terrestrial planets—Earth—Venus. Astrobiology 7(2), 320–332.

INTRODUCTION

The detection and characterization of extrasolar terrestrial planets are the goal of a number of proposed space missions, including the NASA Terrestrial Planet Finders (TPFs) [TPF Coronagraph (TPF-C) and TPF Interferometer (TPF-I)] and the ESA Darwin mission. TPF-I and Darwin are thermal infrared interferometers that use a number of telescopes orbiting in formation and employing the nulling interferometer concept originally suggested by Bracewell (1978). TPF-C is a single visible light telescope that uses a coronagraph. In all cases, the aim of the mis-

Australian Centre for Astrobiology, Macquarie University, Sydney, New South Wales, Australia.

sions is to detect extrasolar terrestrial planets, characterize them, and search for biosignatures. The characterization is carried out by means of spectroscopy.

In this paper, I will review some of the limitations of spectroscopy as a method of characterizing extrasolar terrestrial planets and discuss the possibility of alternative and complementary approaches. In particular, I consider the issue of how well such techniques can detect the presence of liquid water, the defining characteristic of a habitable planet (Hart, 1979; Kasting *et al*., 1993). A habitable planet cannot be recognized simply by its location in the "habitable zone" of a star. The edges of the habitable zone are not well defined and depend on assumptions about the evolution of planetary atmospheres and, hence, the amount of greenhouse heating that will occur. Ideally we need direct observations to characterize the planet's atmosphere and detect habitable conditions.

Spectroscopic techniques cannot detect liquid water on a planet. Spectroscopy, particularly at the low resolution and signal-to-noise ratio that will be feasible on such faint objects, is primarily sensitive to the gaseous components of an atmosphere and not to liquid and solid components that may be present in the atmosphere as clouds and aerosols. The best evidence for a habitable planet, by way of TPF-I or Darwin, would be the simultaneous detection of water vapor bands and a temperature measurement, which would indicate a suitable temperature for liquid water (Des Marais *et al*., 2002). The temperature could be measured from the spectral shape in the thermal infrared region, but this may be problematic in practice in view of the strong molecular absorption bands in this region. In the visible region, water vapor can be detected in the spectrum, but there is no way of measuring the temperature.

There is, however, a technique that is directly sensitive to the presence of liquid droplets in a planet's atmosphere. This is the use of polarization observations as a function of phase angle. Spherical particles (and only liquid droplets are likely to be spherical in natural conditions) produce a strongly polarized peak in scattering at the "primary rainbow" scattering angle (about 139° for water). The feasibility of using this "rainbow scattering" technique as a means of detecting liquid water clouds in a planet's atmosphere is assessed.

Polarization has been used to attempt to detect the scattered light from "hot Jupiter" type extrasolar planets (Hough *et al*., 2006; Lucas *et al*., 2006) and has been suggested as a possible means of detection and characterization of planets with large ground-based telescopes using adaptive optics (Saar and Seager, 2003; Gisler *et al*., 2004; Schmid *et al*., 2006). However, the specific information that can be obtained from the rainbow feature does not seem to have been fully investigated so far.

The paper is organized as follows. First I will discuss the properties of rainbows, and present a series of single scattering calculations of rainbow scattering over a range of particle sizes, shapes, and refractive indices. These results will demonstrate that rainbow scattering is present over the full range of likely cloud droplet sizes and is a strong indicator of liquid droplets. They will also demonstrate that the polarization properties can be used to determine the refractive index and, hence, constrain the nature of the scattering liquid, as well as determine the droplet size. The next section will discuss rainbow scattering in the context of more realistic multiple scattering atmospheres and show how rainbow scattering has been successfully used to determine the nature of liquid droplets in the Venus atmosphere and distinguish liquid droplet clouds from ice clouds in the Earth atmosphere. Then I will discuss the feasibility of observing rainbow scattering in extrasolar terrestrial planets in the context of missions such as TPF-C.

RAINBOWS

Rainbows in ray optics

The formation of a primary rainbow can be understood in the context of ray optics as resulting from light that is internally reflected once inside a spherical liquid droplet (*e.g*., Lynch and Livingston, 2001; Adam, 2002).

If $x = (b/a)$ is the impact parameter b (*i.e*., the minimum distance of the light ray from the droplet center if it was undeflected) normalized by the droplet radius a, then the resulting scattering angle of the light is given by (Adam, 2002):

$$\theta = \pi + 2 \arcsin x - 4 \arcsin (x/n) \qquad (1)$$

where n is the refractive index of the liquid. The scattering angle varies with impact parameter, but the brightest part of the rainbow is a caustic

occurring at the minimum scattering angle, and this occurs at:

$$x_0 = \sqrt{((4 - n^2)/3)} \quad (2)$$

For water, the resulting scattering angle is about 139° (for blue light), which gives a rainbow with a semivertex angle of 41° about the anti-solar point. Light that internally reflects twice inside a droplet gives a secondary rainbow at a scattering angle of about 128°. The region between the primary and secondary rainbows is dark (Alexander's dark band), but some light is scattered into angles inside the primary rainbow and outside the secondary rainbow.

Figure 1 shows the variation of primary rainbow scattering angle with refractive index derived from Eqs. 1 and 2. This variation of scattering angle with refractive index gives rise to the familiar colors of the rainbow since the refractive index of water varies from about 1.344 at 400 nm to 1.329 at 800 nm, which gives a range of scattering angles from 139.5° to 137.4°. It also means that different scattering liquids will give rise to different rainbow angles. Liquid droplet clouds, and probably rain, are known to occur in the atmospheres of Venus and Titan as well as Earth.

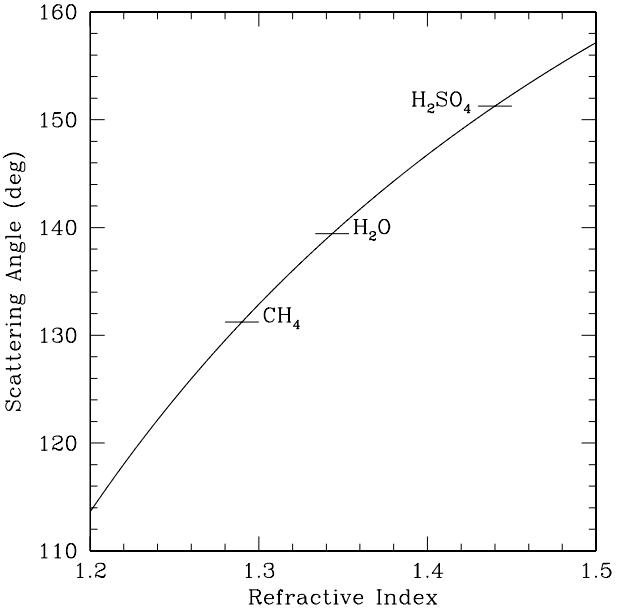

FIG. 1. Primary rainbow scattering angle as a function of refractive index, as determined by the ray optics approximation. The rainbow angles are indicated (at a wavelength of 400 nm) for three substances known to form liquid droplet clouds in the solar system: liquid methane (Titan), water (Earth), and sulfuric acid (Venus).

On Venus, the liquid is sulfuric acid (about 75% H_2SO_4 to 25% H_2O) with a refractive index of 1.44 (Hansen and Hovenier, 1974), whereas on Titan, it is liquid methane at a temperature of ~100K, which has a refractive index of 1.29 (Badoz *et al*., 1992).

The light of the rainbow is highly polarized in a direction perpendicular to the scattering plane. This arises because the angle of incidence within the drop is close to the Brewster angle, at which light with parallel polarization is fully transmitted, but light with perpendicular polarization is partially reflected. For water, the primary rainbow has a polarization of about 96% and the secondary rainbow about 90% for large droplets (Adam, 2002).

Rainbows in Lorenz-Mie theory

The familiar brightly colored rainbows arise from water droplets with a size of 1 mm or larger. However, the rainbow scattering phenomenon persists for much smaller droplets. As the droplets become smaller, diffraction effects broaden the scattering peak (as a function of scattering angle), and this means that rainbows from small droplets (fogbows or cloudbows) no longer show distinct colors. Nevertheless, there is still a strong, highly polarized scattering peak at the primary rainbow angle. It is the ability to observe rainbow scattering from cloud droplets that makes rainbow scattering a feasible technique for studying extrasolar planets.

The rainbow scattering from small particles can be best studied using Lorenz-Mie scattering theory. To investigate the rainbow properties, I have carried out a series of calculations of the normalized scattering matrix F_{ij} (Mishchenko *et al*., 2002, Eq. 4.51) for a size distribution of spherical droplets. The calculations used the code of Mishchenko *et al*. (2002, section 5.10). The size distribution of spherical droplets is specified using the power-law distribution of Hansen and Travis (1974):

$$n(r) = \begin{cases} \text{constant} \times r^{-3}, & r_1 \le r \le r_2, \\ 0, & \textit{otherwise} \end{cases} \quad (3)$$

As described by Mishchenko *et al*. (1997), the values of r_1 and r_2 can be expressed in terms of the cross-section-area weighted effective radius r_{eff} and effective variance v_{eff}.

The components of the normalized scattering matrix describe the intensity and polarization of

the light as a function of scattering angle. F_{11} is the phase function, which describes the angular distribution of the total intensity of the scattered light. F_{12} similarly describes the angular distribution of the linearly polarized light. F_{12}/F_{11} gives the fractional linear polarization of the single scattered light. Both F_{11} and F_{12} are dimensionless.

Figure 2 shows the phase function for scattering from droplets with $r_{\text{eff}} = 200$ μm, a wavelength of 0.4 μm, and two different size distributions. The lower plot has a very narrow size distribution ($v_{\text{eff}} = 0.001$), and the upper plot has a more realistic size distribution with $v_{\text{eff}} = 0.1$. The main features of the rainbow are clearly illustrated here. The primary rainbow and secondary rainbow peaks are separated by Alexander's dark band. Inside the primary rainbow (*i.e.*, at higher scattering angles) are a series of peaks known as the supernumary bows. The spacing of these peaks is dependent on droplet size, so they are only seen clearly for a narrow size distribution, and are smoothed out with the broader distribution.

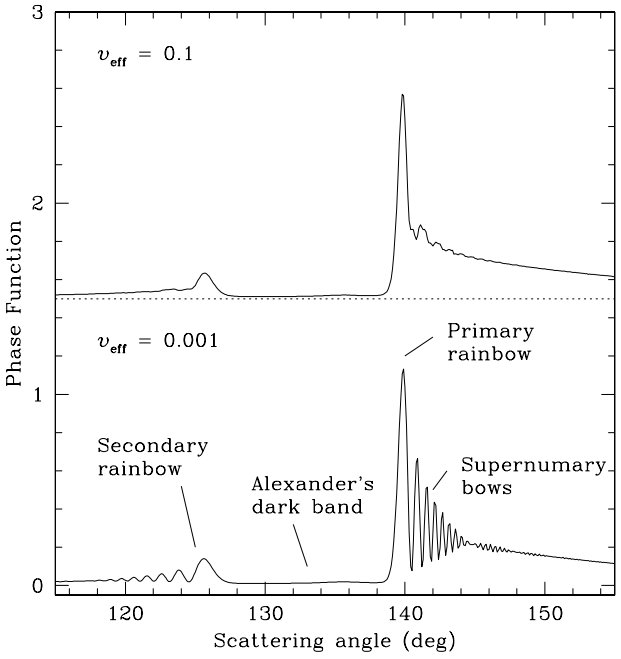

FIG. 2. Lorenz-Mie computations of the phase function for scattering from a size distribution of spherical water droplets with effective radius 200 μm, and effective variance 0.001 (lower plot) and 0.1 (upper plot) at a wavelength of 0.4 μm. The main features of rainbow scattering are indicated. The spacing of the supernumary bows depends on particle size, so these are smoothed out with the broad particle size distribution.

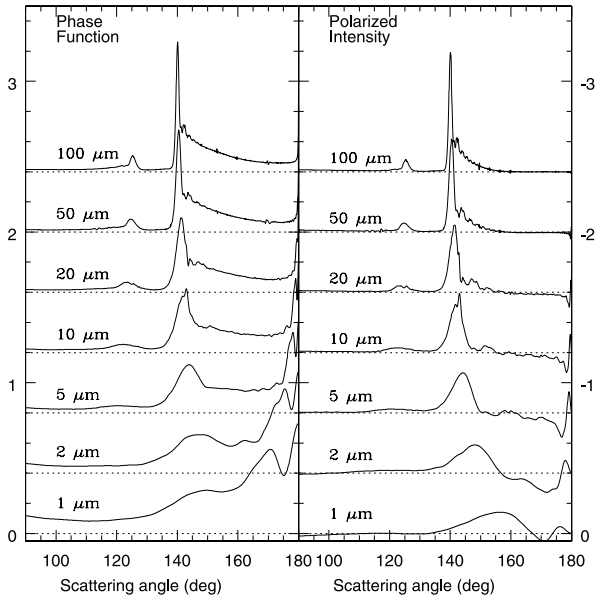

FIG. 3. Lorenz-Mie computations of the effect of droplet size on rainbow scattering. The phase function and polarized intensity for a size distribution of water droplets with effective variance 0.1 at a wavelength of 0.4 μm are plotted for various different effective radii.

Effect of particle size

Figure 3 shows how rainbow scattering varies with particle size. The phase function (F_{11}) and polarized intensity (F_{12}) are plotted as a function of scattering angle. In these and the subsequent plots, F_{11} and F_{12} are plotted on the same scale, so the fact that the rainbow peaks in phase function and polarized intensity reach similar heights indicates that the light is highly polarized. It can be seen that with smaller particle sizes the rainbow peak broadens and shifts to large scattering angles. Features near 180° scattering angle correspond to another scattering phenomenon known as the "glory." At very small particle sizes (~10 μm and less), the rainbow and glory tend to join together in the phase function, and there is no longer a clearly defined edge to the rainbow peak at large scattering angles. However, in polarization the rainbow peak is better defined and can still be seen down to 1 μm particle sizes, though it becomes very broad and shifted.

The calculations here are for a wavelength of 0.4 μm. Since scattering properties are primarily determined by the size parameter, however, these results can be scaled for other wavelengths. For example, 10 μm particles at 0.8 μm wavelength would have almost the same scattering proper-

ties as 5 μm particles at 0.4 μm (apart from the effects of the small change in refractive index with wavelength that will shift the peak).

Remote sensing measurements of liquid water cloud particles in the Earth atmosphere give effective radii ranging from about 3 μm to 30 μm with a global mean value of 11.4 μm (Nakajima *et al.*, 1991; Han *et al.*, 1994). The size of cloud particles in Titan's atmosphere is not well determined, but it is believed that the supersaturation of the atmosphere and lack of nucleation sites will cause rapid growth to large sizes (Lorenz *et al.*, 1993; Griffith *et al.*, 2000). Venus cloud particles in the upper cloud layer show a bimodal size distribution with sizes around 0.6 μm and 2 μm (Esposito *et al.*, 1983). While this is near the lower size limit for rainbow scattering, rainbows are nevertheless clearly observed from Venus, as will be described later.

Thus it is reasonable to believe that rainbow scattering could be expected to occur for most liquid droplet clouds that might be encountered in extrasolar planet atmospheres. In addition, the change in width, and shift, of the rainbow peak with particle size means that an estimate of the particle size can be made from observations of the phase variation of polarization.

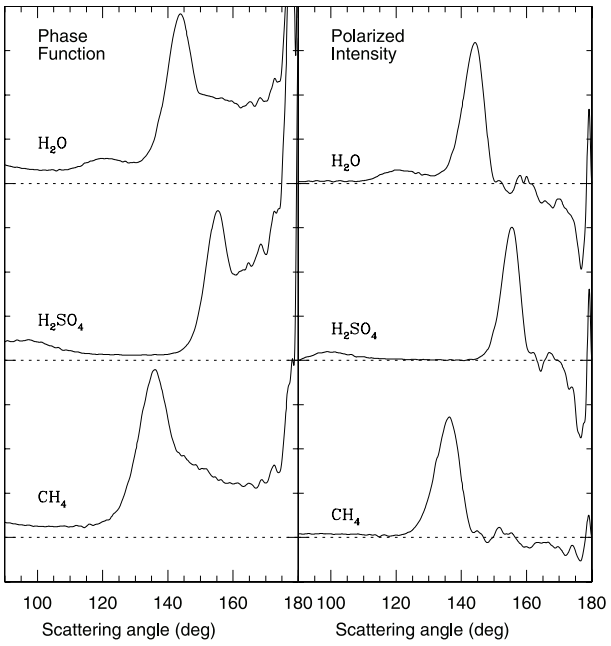

FIG. 4. Lorenz-Mie computations of rainbow scattering for droplets of three liquids known to occur as clouds in the solar system: liquid methane (Titan), water (Earth), and sulfuric acid (Venus). The plots give the phase function and polarized intensity for a size distribution of droplets with effective radius 5 μm and effective variance 0.1 at a wavelength of 0.4 μm.

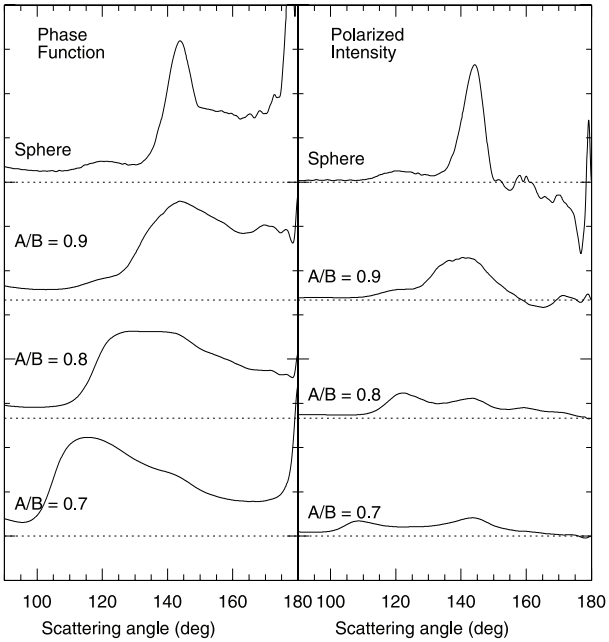

FIG. 5. T-matrix computations showing the effect of particle shape on rainbow scattering. The phase function and polarized intensity for a size distribution of particles with effective radius (of the equivalent surface area sphere) 5 μm and effective variance 0.1 at a wavelength of 0.4 μm are plotted. The refractive index is that of water. The particles are spherical (**top plot**), and then randomly oriented prolate spheroidal particles of different axis ratios. The strong rainbow scattering peak shown by spherical particles becomes much smaller at an axis ratio of 0.9, and largely disappears for even smaller axis ratios.

Effect of refractive index

Figure 4 compares the rainbow scattering properties of the three different liquids known to form liquid droplet clouds in the solar system as described earlier. The calculations are for particles with effective radius 5 μm and effective variance 0.1. It can be seen that the difference in the scattering angle of the primary rainbow clearly separates these three liquids. Thus a measure of the scattering angle of the rainbow peak provides a measure of the refractive index of the liquid responsible. This cannot be considered, on its own, a definitive detection of liquid water, since there are other liquids with similar refractive index. However, in conjunction with other evidence, such as spectroscopic detection of water vapor, it could provide a strong argument that the rainbow was in fact due to liquid water.

Effect of particle shape

Figures 5 and 6 show the effect of particle shape on rainbow scattering. The scattering properties of nonspherical particles are derived using the T-matrix method (Waterman, 1971). The code used here calculates the scattering properties of a size distribution of randomly oriented axially symmetric particles (Mishchenko, 1991; Mishchenko and Travis, 1994; Wielaard *et al*., 1997). The same size distributions are used as for spherical particles. For nonspherical particles, the radius used is that of the equivalent surface-area sphere.

In Fig. 5, the rainbow scattering of spherical water droplets with effective radius 5 μm and effective variance 0.1 at a wavelength of 0.4 μm is compared with that of randomly oriented prolate spheroids with axis ratios of 0.9, 0.8, and 0.7. It can be seen that as the particles depart from sphericity, the rainbow peak rapidly decreases in size. Figure 6 is a similar comparison but with three different particle shapes: a prolate spheroid (as in Fig. 5), an oblate spheroid with axis ratio 1.2, and a cylindrical particle with length equal to its diameter.

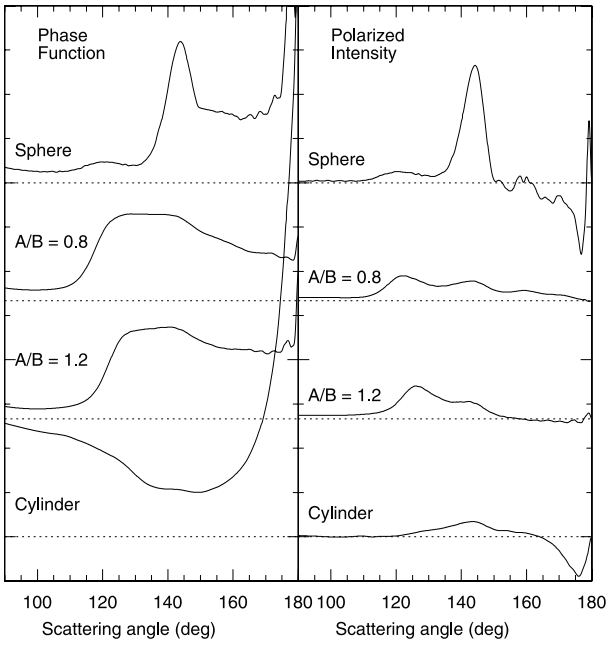

FIG. 6. T-matrix computations showing the effect of particle shape on rainbow scattering. The phase function and polarized intensity for a size distribution of particles with effective radius (of the equivalent surface area sphere) 5 μm and effective variance 0.1 at a wavelength of 0.4 μm are plotted. The refractive index is that of water. The particles are, from top to bottom, spherical particles, randomly oriented prolate spheroidal particles with an axis ratio of 0.8, randomly oriented oblate spheroidal particles with an axis ratio of 1.2, and randomly oriented cylindrical particles with length equal to diameter. The strong rainbow scattering peak shown by spherical particles disappears or is only weakly seen in the nonspherical particles.

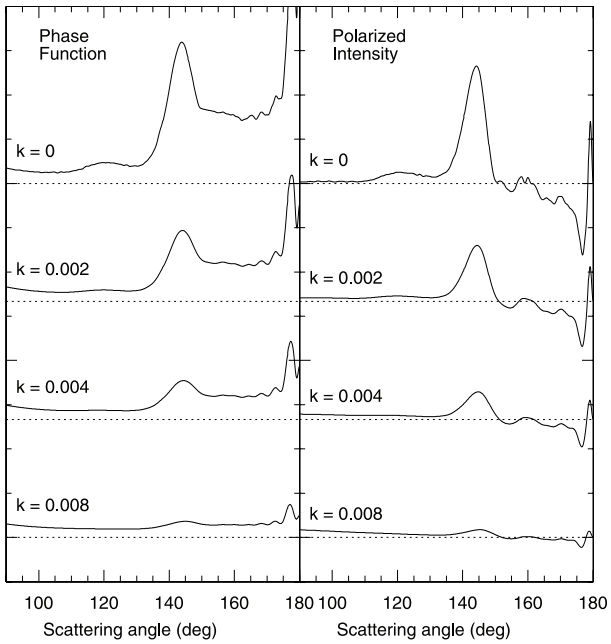

FIG. 7. Lorenz-Mie computations showing the effect of absorption (imaginary component of the refractive index) on rainbow scattering. The phase function and polarized intensity for a size distribution of spherical particles with effective radius 5 μm and effective variance 0.1 at a wavelength of 0.4 μm are plotted. The real refractive index is that of water, and the imaginary part of the refractive index is varied from 0 to 0.008. The strong rainbow scattering peak is reduced in size as the imaginary refractive index increases.

These results show clearly that only spherical particles or particles very close to sphericity will produce a clearly defined rainbow peak.

Effect of absorption

All the previous calculations have assumed nonabsorbing particles (*i.e*., zero imaginary refractive index k). This is a good assumption for water in the visible wavelength range where $k < 10^{-6}$ (Kou *et al*., 1993; Pope and Fry, 1997).

Figure 7 shows the effect on rainbow scattering of adding significant absorption to the particles. The computations are for a size distribution of spherical particles with effective radius 5 μm and effective variance 0.1 at a wavelength of 0.4 μm. The real refractive index is that of water, and

the imaginary refractive index is varied from 0 to 0.008. As the absorption increases the size of the rainbow peak decreases. At $k = 0.002$ it has dropped by about 50% and has largely disappeared by $k = 0.008$.

This means that the polarized flux spectrum of the rainbow scattered light will contain spectral features of the liquid causing the scattering. In principle, this provides a way of more definitively identifying the liquid than is possible from the real refractive index alone. Liquid water has an absorption feature at about 1.95 μm at which k reaches 0.002 (Kou *et al*., 1993). This might, in principle, be observable, but it would be outside the spectral range and beyond the sensitivity of TPF for an Earth-like planet. Absorption features at visible wavelengths are far too weak to be detectable.

Summary of rainbow properties

To summarize the results so far:

- Rainbows are produced by scattering from spherical particles.
- A rainbow scattering peak is present for particle sizes down to about 1 μm for 0.4 μm wavelength.
- The rainbow scattering peak broadens and shifts to higher scattering angles for very small particles.
- Rainbows are highly polarized, and for small particles they are better defined in polarized intensity than in total intensity.
- The scattering angle of the peak rainbow intensity is a measure of the refractive index of the liquid.
- A small departure of the particle from sphericity inhibits the production of a rainbow.
- A small absorption (imaginary refractive index) inhibits the production of a rainbow.

These properties mean that rainbows are strong indicators of liquid droplet clouds. Small liquid droplets are naturally spherical, since surface tension is the dominant force controlling their shape.

Scattering from solid particles in an atmosphere is very unlikely to result in a rainbow, since small size, nonsphericity, absorption, or a combination of these is likely to prevent the occurrence of rainbow scattering. Mineral dust aerosols on Earth are found to have irregular shapes with typical axis ratios of ~1.7 (Okada *et al*., 1987; Nakajima *et al*., 1989). Sulfate aerosols are generally submicron particles and, therefore, too small to form a rainbow. Ice crystals in cirrus clouds have highly nonspherical shapes. Martian atmospheric dust has been found to have effective radius ~1.6 μm and imaginary refractive index k from ~0.005 at 965 nm to ~0.015 at 443 nm (Tomasko *et al*., 1999). These properties would exclude a significant rainbow even if the particles were spherical, which is unlikely to be the case.

RAINBOWS IN MULTIPLE-SCATTERING ATMOSPHERES

The results presented so far are single-scattering calculations. These show a large degree of polarization (~90%) in the rainbow peak. Realistic multiple-scattering atmospheres will not show polarizations this large. To investigate the feasibility of observing rainbows in extrasolar terrestrial planets, we need to determine the size of the rainbow peak in multiple-scattering atmospheres. This can be done by looking at the results of both models and observations.

Multiple-scattering models

In general, the effect of multiple scattering is to suppress polarization, so in a realistic atmosphere the polarized intensity will be dominated by photons that are single-scattered from the top layers of the clouds. A consequence of this is that the shape of the polarized intensity curve calculated for single scattering (as in the previous section) is very similar to what is actually seen from a multiple-scattering atmosphere, in contrast to the situation for total intensity. The additional multiple-scattered light will add unpolarized light that will dilute the polarization and reduce the size of the rainbow peak in the total intensity curve. Hence, in a realistic atmosphere polarization becomes by far the best indicator of rainbow scattering.

Multiple-scattering models of cloud reflectance including polarization have been presented by Hansen (1971) and by Goloub *et al*. (1994). Hansen (1971) showed rainbow peaks with degrees of polarization up to ~20% at near-infrared wavelengths. The height of the peak decreases as the cloud optical thickness increases. Goloub *et al*. (1994) showed that the polarization behavior of

the rainbow peak is better defined if polarized reflectance, rather than degree of polarization, is considered. At a wavelength of 850 nm the polarized reflectance of the rainbow peak reaches a constant value of about 7% for any cloud optical thickness greater than about 1. The total reflectance, however, increases with cloud optical thickness varying from about 30% to 55%. The degree of polarization at the rainbow peak, therefore, ranged from ~13% to ~23%.

Observations of Venus

Venus is a planet with liquid droplet clouds that can be observed through its full range of phase angles from Earth. Polarization observations played an important part in establishing the nature of its clouds. The polarization of Venus was first observed by Lyot (1929) and later studied by Coffeen and Gehrels (1969), Dollfus and Coffeen (1971), Veverka (1971), and others.

Hansen and Arking (1971) used an initial analysis of some of the polarization data to determine that the polarization was consistent with scattering from cloud particles with a radius of about 1 μm and refractive index 1.45 ± 0.02. These results, together with infrared reflectance measurements, led to the independent suggestions by Sill (1972), Young (1973), and Pollack *et al*. (1974) that the Venus clouds were composed of a water solution of sulfuric acid containing at least 75% H_2SO_4.

The definitive analysis of the polarization of Venus was carried out by Hansen and Hovenier (1974). By fitting multiple scattering models to polarization observations at a range of wavelengths, they were able to determine that the cloud particles were spherical droplets with an effective radius of 1.05 μm and refractive index 1.44 ± 0.015 at 0.55 μm. Of many substances previously proposed only sulfuric acid was consistent with the observations. The cloud top pressure was found to be ~50 mbar. These results have been essentially confirmed by *in situ* spacecraft observations, though the size distribution is now known to be more complex than the single size fitted by Hansen and Hovenier (1974).

Because of the large refractive index of sulfuric acid and the small particle size, the primary rainbow was only seen at the shortest wavelengths and found at much larger scattering angles than normally seen for water clouds. The rainbow peak reaches a degree of polarization of ~10% at 0.365 μm, ~6% at 0.445 μm, and ~2.5% at 0.55 μm. The rainbow peak position provided an important constraint on refractive index, which helped to identify the cloud particles as sulfuric acid. Other polarization features such as the glory, anomalous diffraction feature, and Rayleigh scattering are also present.

POLarization and Directionality of Earth Reflectances (POLDER) observations of clouds

The POLDER instrument (Leroy and Lifermann, 2000), developed by the French space agency CNES, flew on the Japanese ADEOS satellite. POLDER measured the angular dependence of the total and polarized reflectance of the Earth from an altitude of 800 km. POLDER uses the polarization measurements to characterize clouds and, in particular, the presence of a rainbow peak in polarized reflectance at ~140° scattering angle to distinguish liquid water clouds from ice clouds (Parol *et al*., 1999; Goloub *et al*., 2000).

The POLDER results confirm that rainbow scattering polarization is observable from clouds in the Earth atmosphere and is a practical tool for detecting liquid water. POLDER also uses Rayleigh scattering polarization as a means by which to determine the cloud-top pressure. The observed polarized reflectances are in reasonable agreement with models (*e.g*., Goloub *et al*., 1994).

Disk-integrated polarization signature of the Earth

A rough estimate of the size of the expected rainbow polarization signature for the disk-integrated Earth can be made as follows. From Goloub *et al*. (1994) the polarized reflectance at the rainbow peak from liquid water clouds is about 7%, and this seems to be in good agreement with observations made with POLDER (*e.g*., Parol *et al*., 1999). Results of the International Satellite Cloud Climatology Project (ISCCP) give a global mean cloud cover of 67.6% (Rossow and Schiffer, 1999). According to ISCCP, this cloud is roughly half liquid water cloud and half ice cloud. However, results from POLDER measurements in February 1997 give 70% liquid clouds and 30% ice clouds (Goloub *et al*., 2000). Since POLDER directly uses the rainbow polarization signature to detect liquid clouds, these results may be most relevant for our purposes. The total reflectance from liquid cloud, ice cloud, and clear regions has

been taken from models used by Tinetti *et al.* (2006, Fig. 8) to fit the Earthshine observations of Woolf *et al*. (2002). These results give reflectances in the visible (0.5–0.8 μm) of ~26% for liquid clouds, ~14% for ice clouds, and ~6% for clear sky. However, these are for a scattering angle of about 118° appropriate to the Earthshine observations. At the rainbow scattering angle of ~142°, the liquid cloud reflectance will be significantly higher. From the cloud reflectance as a function of scattering angle given by Goloub *et al*. (1994), we estimate that this will increase the liquid cloud reflectance to ~35%. The ice cloud and clear sky values have been used unchanged. Cirrus cloud phase functions show little variation with scattering angle over this range (Baran *et al*., 2003). The results are summarized in Table 1.

Zero polarized reflectance is assumed for the ice cloud and clear sky cases. (For the moment other polarization sources such as Rayleigh scattering and ice scattering are ignored. They will contribute some polarization, but POLDER observations show that these contributions are small, and the rainbow peak will clearly stand out in a plot of polarization against scattering angle.) The disk-integrated degree of polarization at the rainbow scattering peak can then be calculated by combining the total and polarized reflectances weighted by their fractions of the global surface area. This gives a polarization of 15.5% using the POLDER cloud phase fractions, and 12.7% using the ISCCP cloud phase fractions. An Earth completely covered by liquid water clouds would have a peak rainbow polarization of 20% under the same assumptions. The peak polarization should not vary much over the 0.5–0.8 μm wavelength range, as both the total reflectances (Tinetti *et al*., 2006) and the size of the rainbow peak (Fig. 3) do not vary strongly with wavelength. At shorter wavelengths, Rayleigh scattering will become significant and cause further dilution that will reduce the height of the rainbow peak.

Table 1. Data Used to Estimate the Disk-Integrated Rainbow Peak Polarization of the Earth

	Global cover		*Reflectance*	
Type	*ISCCP*	*POLDER*	*Total*	*Polarized*
Liquid cloud	33.6%	47.3%	35%	7%
Ice cloud	34.0%	20.3%	14%	0%
Clear sky	32.4%	32.4%	6%	0%

A weighted combination of the reflectances gives a degree of polarization at the rainbow peak of 15.5% for the POLDER cloud phase fractions and 12.7% for the ISCCP cloud phase fractions.

Other polarization features

While this paper concentrates on the polarization due to the rainbow, there are other polarization features from terrestrial planets that can be useful in helping to characterize their atmospheres. In particular, there will be Rayleigh scattering from atmospheric molecules. This will produce a polarization that will peak at a 90° scattering angle and will increase to the blue. The Rayleigh polarization is used by POLDER and in the Venus study described earlier to determine the atmospheric pressure at the cloud top. It can be used in the same way for extrasolar terrestrial planets. Rayleigh scattering provides a good measurement of pressure since all gases contribute to Rayleigh scattering. Pressure cannot easily be estimated from spectra alone, since some potentially important atmospheric constituents, such as N_2, have no absorption features in the TPF ranges (and CO_2 has no strong features in the TPF-C wavelength range). Without a pressure estimate, however, it is difficult to quantitatively interpret the observed absorption features in the spectrum, since for saturated lines (and most features strong enough to be detected with TPF are likely to have saturated lines), the observed band strength depends on the amount of pressure broadening as well as on the column density of the absorber. While Rayleigh scattering may be detectable in the intensity spectrum as a rise to blue wavelengths, its polarization signature would provide a much more definitive measurement.

Polarization will also arise from scattering due to solid particles in the atmosphere such as ice or dust. While these do not produce rainbows, the variation of polarization with phase angle may still provide valuable information that will help to constrain particle composition and size.

Limitations

The techniques described here tell us about conditions at the planet's cloud top. The detection of liquid water at the cloud top does not necessarily imply that the planet will have habitable conditions at its surface. On Venus, for example, the conditions at the surface are very different from those at the cloud top. This limitation is in-

herent in TPF-type missions that work at wavelengths that cannot penetrate the clouds.

However, polarimetric observations would help to distinguish a Venus-like planet from an abiotic cloudy Earth, since the Venus sulfuric acids clouds give a very different polarization signature to water clouds on Earth. The Venus rainbow, which occurs at high phase angle and is limited to short wavelengths, would be hard to detect with TPF-C sensitivities. Such a planet would, therefore, come up negative in a search for water rainbow scattering. At higher sensitivity, it might be possible to detect the sulfuric acid rainbow and determine the true nature of the clouds.

FEASIBILITY OF OBSERVING RAINBOWS IN EXTRASOLAR TERRESTRIAL PLANETS

From the previous section, we estimate that a terrestrial planet with liquid water clouds should show a well-defined peak in polarization at about scattering angle 140° (phase angle 40°) with degree of linear polarization reaching 10–20% at the peak. Detection of such a peak would require polarization measurements covering a range of phase angle around the peak (say, 30–50°).

The first requirement is that we must be able to observe the planet at the required phase angles. This will not always be possible, as planets with face-on orbits will never reach these phase angles. To reach the 40° phase angle, the orbital inclination needs to be at least 50°, and to reach the 30° phase angle, at least 60°.

For randomly oriented orbits, the probability of an inclination greater than i is equal to cos i. Thus, 64% of systems would reach the rainbow phase angle, and 50% of systems would reach 30° phase angle and, thus, allow us to observe both sides of the rainbow peak. If, however, any prior selection of systems is carried out based on previous detection of planets using Doppler or transit techniques, then the fraction could be much higher, as these detection techniques are biased toward finding planets at high inclinations.

Another issue is that observing a planet at the rainbow phase angle requires observations at less than its maximum separation from the star. For a circular orbit, the maximum separation from the star occurs at phase angle 90°. To observe the primary rainbow, the planet has to be observed at a separation smaller by a factor sin θ for phase angle θ. Thus, the separation from the star will be 0.64 of its maximum at 40° phase angle and 0.5 of its maximum at 30°. If the instrument has a minimum angle from the star at which it can operate, this may limit the number of planets for which such observations are possible.

In cases where such observations are possible, however, there are considerable advantages in observing planets at these phase angles. Figure 8 shows the light curve of Venus (Mallama *et al.*, 2006). The data are corrected to a constant distance of 1 astronomical unit and then normalized to a value of 1 at full phase. The variation with phase is a combination of the change in illuminated area of the disk, together with the angular dependence of scattering from clouds. The planet is 2.6 times brighter at the 40° water rainbow phase angle than at a phase angle of 90°. Scattering from clouds on earth shows a similar increase in brightness with phase angle (Goloub *et al.*, 2004). Such a phase angle may well be close to optimum for any characterization observations of these planets, being a good compromise between the increasing brightness of the planet at smaller

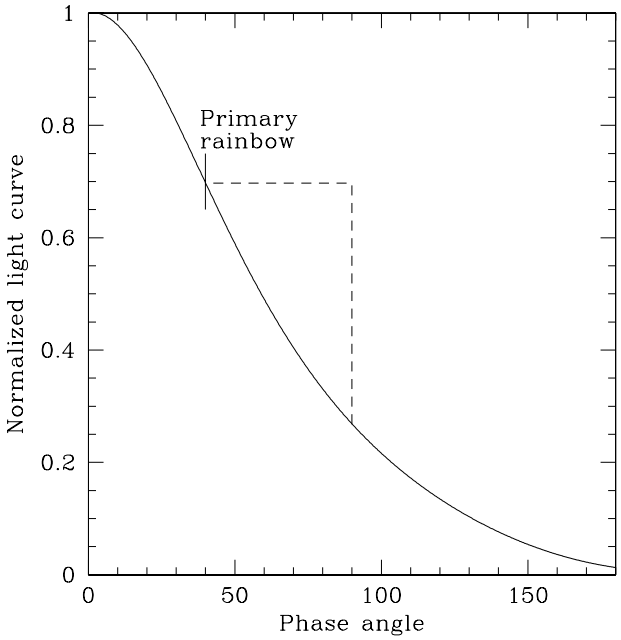

FIG. 8. Polynomial fit to photometry of the planet Venus, corrected to a constant distance of 1 astronomical unit, and normalized to one at full phase. At the water primary rainbow phase angle (~40°) the planet is 2.6 times brighter than it is at 90° phase angle (corresponding to maximum separation from the star for an extrasolar planet).

phase angles and the decreasing separation from the star.

Any characterization observations of extrasolar terrestrial planets are going to be challenging in view of the extreme faintness of the planets, and are likely to require very long integrations. However, an advantage of polarimetry over spectroscopy is that broad wavelength band observations can be used, as the rainbow peak should persist over a wide wavelength range. To detect polarization peaks with heights of ~10–20%, polarization measurements to an accuracy of about 2% would be needed. In the photon-noise limited case, this requires detection of ~2,500 photons over the broad band. To detect the peak, observations at about six carefully chosen phase angles would be needed. Thus, a total of 15,000 photons are needed. This can be compared with requirements for spectroscopic characterization. Detection of the spectral features in the visible would require observations with a spectral resolving power $R \sim 100$ and a signal-to-noise ratio of about 20. This gives 46 spectral resolution elements over a 0.5–0.8 μm wavelength range, and 400 photons required in each element, a total of ~18,000 photons. Thus, the photon requirement and, hence, total integration time for polarimetric characterization and spectroscopic characterization are about the same.

However, there is no need to make separate polarization and spectroscopic observations. An appropriately designed instrument could measure the polarization in each wavelength bin and combine the data to give broad-band polarization as a function of phase angle, as well as the combined spectrum. In this way, polarization and spectroscopic data could be obtained with minimal increases in the total integration time compared with just obtaining the spectroscopic data.

The design of the TPF-C optical system (Dooley and Lawson, 2005) seems to allow relatively straightforward incorporation of polarimetry, since it uses a polarizing beamsplitter followed by two identical light paths each of which contain a wavefront corrector and coronograph. The use of identical instruments on each beam, combined with careful calibration, may be sufficient to obtain the polarization measurements. This would mean that no further beam splitting or additional detectors would be needed. TPF-C uses an off-axis optical system, and this will introduce some telescope polarization. It should be straightforward to correct for this, however, given that the polarimetric precision required for rainbow detection (~1%) is relatively undemanding [polarization measurement to parts in 10^6 are being achieved in ground-based astronomy (Lucas *et al.*, 2006)]. A further important issue will be the background exozodiacal light. This will also be polarized, and therefore accurate background subtraction will be essential.

CONCLUSIONS

Scattering from liquid droplet clouds in a planet's atmosphere produces a strongly polarized peak at the rainbow scattering angle (about 140° for liquid water). The presence of such a peak is a strong indicator of liquid clouds, and the scattering angle of the peak polarization is dependent on the refractive index and, thus, constrains the nature of the liquid. No such peak is likely to occur for solid scattering particles such as aerosols or ice clouds. Observations of the rainbow feature, and other polarization effects, could complement spectroscopic observations and improve our capability to characterize the atmospheres of extrasolar terrestrial planets.

The disk-integrated degree of polarization at the rainbow peak, at visible wavelengths, is estimated to be 12.7% or 15.5% for two models of the Earth's cloud cover, and would be about 20% for an Earth totally covered with liquid water cloud.

The polarization signal could be measured with a telescope such as TPF-C in similar total integration times to those required for spectroscopic characterization. Since spectroscopy and polarimetry could be obtained simultaneously with the same instrument, this additional information could be obtained with minimal additional integration time compared with purely spectroscopic characterization.

Polarization needs to be included in future multiple-scattering models of extrasolar planet atmospheres in that it will allow improved calculations of the size of the rainbow peak and other polarization phenomena.

ABBREVIATIONS

ISCCP, International Satellite Cloud Climatology Project; POLDER, POLarization and Directionality of Earth Reflectances; TPF, Terrestrial Planet Finder; TPF-C, Terrestrial Planet Finder

Coronograph; TPF-I, Terrestrial Planet Finder Interferometer.

REFERENCES

Adam, J.A. (2002) The mathematical physics of rainbows and glories. *Phys. Rep.* 356(4), 229–365.

Badoz, J., Le Liboux, M., Nahoum, R., Istrael, G., Raulin, F., and Torre, J.P. (1992) A sensitive cryogenic refractometer. Application to the refractive index determination of pure or mixed liquid methane, ethane, and nitrogen. *Rev. Sci. Instrum.* 63(5), 2967–2973.

Baran, A.J., Havemann, S., Francis, P.N., and Watts, P.D. (2003) A consistent set of single-scattering properties for cirrus cloud: tests using radiance measurements from a dual-viewing multi-wavelength satellite-based instrument. *J. Quant. Spect. Rad. Trans*. 79-80, 549–567.

Bracewell, R. (1978) Detecting nonsolar planets by spinning infrared interferometer. *Nature* 274(5673), 780–781.

Coffeen, D.L. and Gehrels, T. (1969) Wavelength dependence of polarization. XV. Observations of Venus. *Astron. J.* 74(3), 433–445.

Des Marais, D.J., Harwitt, M.O., Jucks, K.W., Kasting, J.F., Lin, D.N.C., Lunine, J.I., Schneider, J., Seager, S., Traub, W.A., and Woolf, N.J. (2002) Remote sensing of planetary properties and biosignatures on extrasolar terrestrial planets. *Astrobiology* 2(2), 153–181.

Dollfus, A. and Coffeen, D.L. (1970) Polarization of Venus. I. Disk observations. *Astron. Astrophys*. 8, 251–266.

Dooley, J.A. and Lawson, P.R. (2005) *Technology Plan for the Terrestrial Planet Finder Coronagraph*, JPL Publication 05-8, Jet Propulsion Laboratory, Pasadena, CA.

Esposito, L.W., Knollenberg, R.G., Marov, M.Ya., Toon, O.B. and Yurco, R.P. (1983) The clouds and hazes of Venus. In *Venus*, edited by D.M. Hunten, L. Colin, T.M. Donahue, and V.I. Moroz, University of Arizona Press, Tucson, pp. 484–564.

Gisler, D., Schmid, H.M., Thalmann, C., Povel, H.P., Stenflo, J.O., Joos, F., Feldt, M., Lenzen, R., Tinbergen, J., Gratton, R., Stuik, R., Stam, D.M., Brandner, W., Hippler, S., Turratto, M., Neuhauser, R., Dominik, C., Hatzes, A., Henning, T., Lima, J., Quirrenbach, A., Waters, L.B.F.M., Wuchertl, G., and Zinnecker, H. (2004) CHEOPS/ZIMPOL: a VLT instrument study for the polarimetric search of scattered light from extrasolar planets. *SPIE Proc*. 5492, 463–474.

Goloub, P., Deuze, J.L., Herman, M., and Fouquart, Y. (1994) Analysis of the POLDER polarization measurements performed over cloud covers. *IEEE Trans. Geosci. Remote Sensing* 3(1), 78–88.

Goloub, P., Herman, M., Chepfer, H., Riedi, J., Brogniez, G., Couvert, P., and Seze, G. (2000) Cloud thermodynamical phase classification from the POLDER spaceborne instrument. *J. Geophys. Res*. 105(D11), 14747–14759.

Griffith, C.A., Hall, J.F., and Geballe, T.R. (2000) Detection of daily clouds on Titan. *Science* 290(5491), 509–513.

Han, Q., Rossow, W.B., and Lacis, A.S. (1994) Near-global survey of effective droplet radii in liquid water clouds using ISCCP data. *J. Climate* 7(4), 465–497.

Hansen, J.E. (1971) Multiple scattering of polarized light in planetary atmospheres. Part II. Sunlight reflected by terrestrial water clouds. *J. Atmos. Sci*. 28(8), 1400–1426.

Hansen, J.E. and Arking, A. (1971) Clouds of Venus: evidence for their nature. *Science* 171(3972), 669–672.

Hansen, J.E. and Hovenier, J.W. (1974) Interpretation of the polarization of Venus. *J. Atmos. Sci*. 31(4), 1137–1160.

Hansen, J.E. and Travis, L.D. (1974) Light scattering in planetary atmospheres. *Space Sci. Rev*. 16, 527–610.

Hart, M.H. (1979) Habitable zones about main sequence stars. *Icarus* 37(1), 351–357.

Hough, J.H., Lucas, P.W. and Bailey, J. (2006) The polarization signature of extra-solar planets. In *IAU Symposium 232: Scientific Requirements for Extremely Large Telescopes*, edited by P. Whitelock, M. Dennefeld, and B. Leibundgut, Cambridge University Press, Cambridge, UK, pp. 350–355.

Kasting, J.F., Whitmire, D.P., and Reynolds, R.T. (1993) Habitable zones around main sequence stars. *Icarus* 101(1), 108–128.

Kou, L., Labrie, D., and Chylek, P. (1993) Refractive indices of water and ice in the 0.65- to 2.5 μm spectral range. *Appl. Opt*. 32(19), 3531–3540.

Leroy, M. and Lifermann, A. (2000) The POLDER instrument onboard ADEOS: scientific expectations and first results. *Adv. Space Res*. 25(5), 947–952.

Lorenz, R.D. (1993) The life, death and afterlife of a raindrop on Titan. *Planet. Space Sci*. 41(9), 647–655.

Lucas, P.W., Hough, J.H., and Bailey, J.A. (2006) PLANETPOL: polarimetry of hot Jupiters at the parts per million level. In *Tenth Anniversary of 51 Peg-b: Status of and Prospects for Hot Jupiter Studies*, edited by L. Arnold, F. Bouchy, and C. Moutou, Frontier Group, Paris, France, pp. 334–341.

Lynch, D.K. and Livingston, W. (2001) *Color and Light in Nature*, Cambridge University Press, Cambridge, UK, pp. 109–121.

Lyot, B. (1929) Recherches sur la polarisation de la lumiere des planets et de quelques substances terrestres. *Ann. Observ. Paris (Meudon)* 8(1), 1–161.

Mallama, A., Wang, D., and Howard, R.A. (2006) Venus phase function and forward scattering from H_2SO_4. *Icarus* 182(1), 10–22.

Mishchenko, M.I. (1991) Light scattering by randomly oriented axially symmetric particles. *J. Opt. Soc. Am. A* 8(6), 871–882.

Mishchenko, M.I. and Travis, L.D. (1994) T-matrix computations of light scattering by large spheroidal particles. *Opt. Commun*. 109(1-2), 16–21.

Mishchenko, M.I., Travis, L.D., Kahn, R.A., and West, R.A. (1997) Modeling phase functions for dustlike tropospheric aerosols using a shape mixture of randomly oriented polydisperse spheroids. *J. Geophys. Res*. 102 (D14), 16831–16847.

Mishchenko, M.I., Travis, L.D., and Lacis, A.A. (2002) *Scattering, Absorption and Emission of Light by Small Particles*, Cambridge University Press, Cambridge, UK.

Nakajima, T.M., Tanaka, M., Yamano, M., Shiobara, M., Arao, K., and Nakanishi, Y. (1989) Aerosol optical characteristics in the yellow sand events observed in May 1982 at Nagasaki. II. Models. *J. Meteorol. Soc. Jpn*. 67(2), 279–291.

Nakajima, T., King, M.D., Sphinhire, J.D., and Radke, L.F. (1991) Determination of optical thickness and effective particle radius from reflected solar radiation measurement. Part II: Marine stratocumulus observations. *J. Atmos. Sci*. 48(5), 728–750.

Okada, K., Kobayashi, A., Iwasaka, Y., Naruse, H., Tanaka, T., and Nemoto, O. (1987) Features of individual asian dust-storm particles collected at Nagoya, Japan. *J. Meteorol. Soc. Jpn*. 65(3), 515–521.

Parol, F., Buriez, J.-C., Vanbauce, C., Couvert, P., Seze, G., Goloub, P., and Chinet, S. (1999) First results from the POLDER "Earth Radiation Budget and Clouds" operational algorithm. *IEEE Trans. Geosci. Rem. Sensing* 37(3), 1597–1612.

Pollack, J.B., Erickson, E.F., Witteborn, F.C., Chackerian, C., Summers, A.L., van Camp, W., Baldwin, B.J., Augason, G.C., and Caroff, L.J. (1974) Aircraft observations of Venus' near-infrared reflection spectrum—implications for cloud composition. *Icarus* 23(1), 8–26.

Pope, R.M. and Fry, E.S. (1997) Absorption spectrum (380–700 nm) of pure water. II. Integrating cavity measurements. *Appl. Opt*. 36(33), 8710–8723.

Rossow, W.B. and Schiffer, R.A. (1999) Advances in understanding clouds from ISCCP. *Bull. Am. Meteorol. Soc*. 80(11), 2261–2287.

Saar, S.H. and Seager, S. (2003) Uses of linear polarization as a probe of extrasolar planet atmospheres. In *ASP Conference Series, Vol. 294*: *Scientific Frontiers in Research on Extrasolar Planets*, edited by D. Deming and S. Seager, Astronomical Society of the Pacific, San Francisco, pp. 529–534.

Schmid, H.M., Beuzit, J.-L., Feldt, M., Gisler, D., Gratton, R., Henning, Th., Joos, F., Kasper, M., Lenzen, R., Mouillet, D., Moutou, C., Quirrenbach, A., Stam, D.M., Thalmann, C., Tinbergen, J., Verinaud, C., Waters, R., and Wolstencroft, R. (2006) Search and investigation of extra-solar planets with polarimetry. In *IAU Colloquium 200: Direct Imaging of Exoplanets: Science and Techniques*, edited by C. Aime and F. Vakili, Cambridge University Press, Cambridge, UK, pp. 165–170.

Sill, G.T. (1972) Sulfuric acid in the Venus clouds. *Commun. Lunar Planet Lab*. 9, 191–198.

Tinetti, G., Meadows, V.S., Crisp, D., Fong, W., Fishbein, E., Turnbull, M., and Bibring, J.-B. (2006) Detectability of planetary characteristics in disk-averaged spectra. I: The Earth model. *Astrobiology* 6(1), 34–47.

Tomasko, M.G., Doose, L.R., Lemmon, M., Smith, P.H., and Wegryn, E. (1999) Properties of dust in the Martian atmosphere from the Imager on Mars Pathfinder. *J. Geophys. Res.* 104(E4), 8987–9007.

Veverka, J. (1971) A polarimetric search for a Venus halo during the 1969 inferior conjunction. *Icarus* 14(2), 282–283.

Waterman, P.C. (1971) Symmetry, unitarity, and geometry in electromagnetic scattering. *Phys. Rev. D* 3, 825–839.

Wielaard, D.J., Mishchenko, M.I., Macke, A., and Carlson, B.E. (1997) Improved T-matrix computations for large nonabsorbing and weakly absorbing nonspherical particles and comparison with geometrical-optics approximation. *Appl. Opt*. 36(18), 4305–4313.

Woolf, N.J., Smith, P.S., Traub, W.A., and Jucks, K.W. (2002) The spectrum of earthshine: a pale blue dot observed from the ground. *Astrophys. J*. 574(1), 430–433.

Young, A.T. (1973) Are the clouds of Venus sulfuric acid? *Icarus* 18(4), 564–582.

Address reprint requests to:
Jeremy Bailey
Australian Centre for Astrobiology
Macquarie University
Sydney, NSW 2109, Australia

E-mail: jbailey@els.mq.edu.au

This article has been cited by:

1. D. M. Stam. 2008. Spectropolarimetric signatures of Earth-like extrasolar planets. *Astronomy and Astrophysics* **482**:3, 989-1007. [CrossRef]